Analytical Methods

PAPER

View Article Online
View Journal

Cite this: DOI: 10.1039/c8ay02150c

Gold nanoparticle decorated multiwalled carbon nanotube modified electrodes for the electrochemical determination of theophylline†

Wanderson da Silva, Mariana Emilia Ghica and Christopher M. A. Brett *

A novel and easy to prepare electrochemical sensor for theophylline (TP) determination was developed based on a new conductive platform prepared by direct dispersion of gold nanoparticles (AuNP) on a multiwalled carbon nanotube (MWCNT) network prior to deposition on a glassy carbon electrode (GCE). Cyclic voltammetry, differential pulse voltammetry, and electrochemical impedance spectroscopy were used to characterize the system. The modified electrode (AuNP-MWCNT/GCE) exhibited good promotion of the electrochemical oxidation of TP, factors such as solution pH, amount of MWCNT, and accumulation time and potential being optimised. Under the best conditions, the oxidation peak current of TP was linearly proportional to concentration in the range 0.5–20 μM and the limit of detection (LOD) was estimated to be 90 nM. The developed method showed good reproducibility and excellent selectivity. Furthermore, the sensor was successfully applied to the determination of TP in pharmaceutical tablets and tea samples with excellent recoveries.

Received 1st October 2018
Accepted 8th November 2018

DOI: 10.1039/c8ay02150c

rsc.li/methods

1. Introduction

Metallic nanomaterials have attracted considerable attention due to their unique optical, electrical, and catalytic properties.[1] Among them, those of Au, Pt, Ag, Co, Ni, Cu, and Fe have been extensively used in sensor technology owing to their inherent properties, such as electrocatalytic activity, conductivity, stability, biocompatibility and large surface area, which allow their applicability as modifier agents on electrode surfaces for sensors and biosensors.[2,3] Gold nanoparticles (AuNP), in particular, are of great interest because, in addition to properties common to all nanoparticles, the attachment or incorporation of AuNP into thin films enhances the electron transfer between redox centres and electrode surfaces and make them an ideal material for sensor applications. Their special electronic properties with a high surface-to-volume-ratio are responsible for their excellent electrocatalytic activity in a variety of chemical reactions.[4,5] When metallic nanoparticles are combined with other nanostructures such as carbon nanotubes (CNT), the performance of the final composite material can be further improved, since carbon nanotube–metal composites have the individual properties of both constituent components as well as a synergistic effect that can be exploited in modified electrodes.[6–8] The use of AuNP–CNT nanocomposites offers several advantages, such as easy surface modification, as well as excellent conductivity[8] and increased sensitivity and selectivity through their ability to separate the oxidation potentials of different analytes.[9–11] In this regard, a number of metal nanoparticle/carbon nanotube substrate hybrid nanostructures have been used as sensitive modified electrodes for different analytes.[12–14]

Theophylline (TP) is a xanthine derivative commonly utilized as a clinical drug for the treatment of respiratory system diseases such as bronchial asthma and other bronchospastic conditions due to its capability of relieving bronchospasms.[15] TP induces bronchodilation and is used as an expectorant. Nevertheless, TP has to be monitored clinically to avoid serious toxicological effects because it exhibits a narrow safety range of 5–20 μg mL^{-1} (27–111 μmol L^{-1}). Nowadays, measurements of serum TP are carried out routinely using methods such as high-performance liquid chromatography,[16,17] gas chromatography,[18] spectroscopic methods[19,20] and electrochemical methods.[21] Among these methods, electrochemical methods can show remarkable advantages mainly due to the simplicity, sensitivity, selectivity, low cost and relatively short analysis time compared with other techniques.[22]

For electrochemical analysis, the key component is electrode modification, which requires the selection of suitable materials to improve the analytical performance. To date, many materials have been synthesized and used as electrode modifier materials for TP detection, among them MWCNT, graphene, polymers and nanoparticles.[23] To our knowledge, the combination of carbon nanotubes and gold nanoparticles as electrode

Department of Chemistry, Faculty of Sciences and Technology, University of Coimbra, 3004-535 Coimbra, Portugal. E-mail: cbrett@ci.uc.pt; Fax: +351-239827703; Tel: +351-239854470

† Electronic supplementary information (ESI) available. See DOI: 10.1039/c8ay02150c

modifiers for theophylline detection has only been reported in combination with poly-L-lysine.[24]

In the present work, a simpler electrode configuration has been prepared without poly-L-lysine or other aggregation agent, consisting of gold nanoparticles dispersed in a multiwalled carbon nanotube–chitosan network, deposited in one step on a glassy carbon electrode substrate. Cyclic voltammetry (CV) and electrochemical impedance spectroscopy (EIS) were used for characterization of the modified electrode and differential pulse voltammetry (DPV) for analytical determination of TP. The morphology and distribution of the nanostructures were examined by surface characterisation with transmission and scanning electron microscopy. Optimization of the parameters influencing theophylline's analytical determination are discussed and application to commercial drug and tea samples is demonstrated.

2. Experimental

2.1. Reagents and solutions

All reagents were of analytical grade and used without further purification. Theophylline, anhydrous (purity ≥ 99.00%), gold(III) chloride hydrate (purity ≥ 99.99%), chitosan from crab shells, minimum 85% deacetylated, were purchased from Sigma-Aldrich. Sodium citrate, dehydrate (purity ≥ 99.00%) was from Merck, Germany. Multiwalled carbon nanotubes (MWCNT) with ~95% purity, 30 ± 10 nm diameter, and 1–5 μm length were from Nanolab, U.S.A. For the electrochemical experiments, the supporting electrolyte Britton–Robison (BR) buffer was prepared by mixing phosphoric acid, acetic acid and boric acid (all solutions of 0.04 M) and adjusting the pH with sodium hydroxide (0.2 M). Millipore Milli-Q nanopure water (resistivity ≥ 18 MΩ cm) was used for the preparation of all solutions. All experiments were performed at room temperature (25 ± 1 °C).

2.2. Instrumentation

A scanning electron microscope (SEM) (JEOL, JSM-5310, Japan) was used for the characterization of the AuNP and transmission electron microscope (TEM) images were recorded using a JEOL JEM-1230 for characterization of the nanocomposite surface.

Voltammetric experiments were carried out with a computer controlled Ivium Compact Stat, in a one-compartment three electrode system. This consisted of a glassy carbon electrode (GCE) (geometric area 0.00785 cm^2, Bio-Logic, France), a GCE modified with metallic gold nanoparticles (AuNP), with MWCNT, or with metallic gold nanoparticles dispersed in a multiwalled carbon nanotube network (AuNP–MWCNT) as working electrode, a platinum wire as counter electrode and an Ag/AgCl (3 M KCl) as reference electrode.

Electrochemical impedance measurements were carried out with a Solartron 1250 Frequency Response Analyser coupled to a Solartron 1286 Electrochemical Interface using ZPlot 2.4 software (Solartron Analytical, UK). A sinusoidal voltage perturbation of amplitude 10 mV rms was applied in the frequency range between 65 kHz and 0.01 Hz with 10 frequency steps per decade.

The pH measurements were made with a CRISON 2001 micro pH-meter.

2.3. Preparation of the modified electrodes

Metallic gold nanoparticles were synthesized by reduction of $HAuCl_4 \cdot H_2O$ with sodium citrate as follows. A volume of 200 mL of a solution of 0.01% $HAuCl_4$ in water was brought to boiling point, to which 7.0 mL of 1.0% sodium citrate was slowly added under stirring[25] and left to react for 10 min. The resulting gold nanoparticle dispersion was then purified in order to remove the remaining traces of sodium citrate and unreacted $HAuCl_4$ by centrifugation at 14 000 rpm for 20 min followed by redispersion of the precipitated solid in 200 mL of Milli-Q water. Prior to glassy carbon electrode modification, it was polished on a metallographic pad successively with diamond sprays of particle size of 6 μM, 3 μM and 1 μM (Kemet, UK). It was then rinsed with Milli-Q water and sonicated during 30 s for removing any particles adhering to the electrode surface. Functionalized MWCNT were obtained by treating the MWCNT in 3 M HNO_3 under continuous stirring for 24 h, afterwards being thoroughly washed with Milli-Q water and dried at 80 °C for 12 h.[26] Different suspensions of MWCNT were prepared: 0.2, 0.5 and 1.0 w/v% in 1% (w/v) chitosan dissolved in 1% (v/v) acetic acid and sonicated for 4 h until homogenization. In order to prepare AuNP–MWCNT composite, the dispersions of MWCNT in chitosan (0.2, 0.5 and, 1.0 w/v%) were mixed with equal volumes of the gold nanoparticle stock solution prepared previously, designated AuNP–$MWCNT_{0.10}$, AuNP–$MWCNT_{0.25}$, and AuNP–$MWCNT_{0.50}$. The mixture was sonicated for 2 h and then kept at rest for 24 h before use, in order to facilitate the aggregation of gold nanoparticles in the MWCNT network. These dispersions were used for drop-casting of 2 μL on the GCE surface. AuNP/GCE and $MWCNT_{0.25}$/GCE modified electrodes were also prepared by the same procedure. The modified electrodes were left to dry at room temperature for 24 h before further use.

2.4. Sample preparation and analysis

In order to evaluate the applicability of the new electrode configuration in real sample analysis, TP was measured in pharmaceutical tablets and in two types of tea (green and black tea) using the standard addition method. The samples were prepared as described below.

One TP pharmaceutical tablet, labelled with 400 mg TP per tablet, was accurately weighted and grounded into powder in an agate mortar. The TP powder was dissolved in 100 mL of deionized water and used for determination.

For the tea samples, 5 g of each tea was boiled in 60 mL of deionized water for 20 min in order to extract the theophylline. After filtration, the filtrate was collected and deionized water added up to a final volume of 100 mL.

3. Results and discussion

3.1. Characterization of nanostructures

The size, shape, and distribution of the AuNP were visualized by SEM and the aggregation of the nanoparticles on the carbon nanotube network was also verified by SEM and TEM. The SEM image of the AuNP, Fig. 1A shows nanoparticles with an excellent dispersibility and also exhibiting a homogeneous surface and uniform spherical morphology. The controlled size of the

nanoparticles plays an important role as they are able to enhance significantly the electrochemical conductivity of the nanocomposite as compared with non-dispersed or non-homogenous nanoparticles.[27] The size distribution of the AuNP was analyzed by ImageJ open source particle analysis software, in which 500 discreet nanoparticles were used as sample space. From the particle size Gaussian distribution curve, Fig. 1B, the average size of the AuNP was calculated as 18.6 ± 0.5 nm. SEM and TEM were also used to confirm the formation of the nanocomposite and for evaluating the dispersion of AuNP on the MWCNT network, Fig. 1C and D. AuNP are well distributed in the MWCNT network with nanoparticles attached to the walls of the carbon nanotubes in a compact manner, Fig. 1C. This proves the formation of the nanocomposite and shows that the new methodology for depositing nanoparticles on carbon nanotube networks was successfully performed. Cyclic voltammetry with the modified AuNP–MWCNT$_{0.25}$/GCE in acidic media also confirmed the presence of gold on the carbon nanotubes, see ESI, Fig. S1.† A small oxidation peak, II$_a$, is observed, which can be ascribed to gold oxide formation. The corresponding reduction peak is coincident with that of the MWCNT reduction peak I$_c$.

3.2. Characterization of the modified electrodes

Unmodified and modified GCE with different architectures: gold nanoparticles (AuNP/GCE), carbon nanotubes (MWCNT$_{0.25}$/GCE) and gold nanoparticles–carbon nanotubes (AuNP–MWCNT$_{0.25}$/GCE) were characterized by cyclic voltammetry (CV) and electrochemical impedance spectroscopy (EIS) in the presence of theophylline.

3.2.1. Cyclic voltammetry. Fig. 2 shows cyclic voltammograms at modified and unmodified GCE in 250 μM TP prepared in 0.1 M BR buffer (pH 6.0) in the potential range of +0.5 – +1.4 V, with a scan rate of 100 mV s^{-1}. One oxidation peak appears at +1.11 V for GCE and AuNP/GCE, at +1.05 V for MWCNT$_{0.25}$/GCE and at +0.98 V for AuNP–MWCNT$_{0.25}$/GCE and there is no reduction peak on the reverse scan, indicating that the oxidation process of TP at bare and modified electrodes is irreversible. Thus, the potential shifts 130 mV to a less positive value, corresponding to a significant electrocatalytic effect at AuNP–MWCNT$_{0.25}$/GCE, accompanied by a peak current enhancement compared with bare GCE. At AuNP–MWCNT$_{0.25}$/GCE, the response to TP increased by a factor of 60 compared with a bare electrode, while at MWCNT$_{0.25}$/GCE and AuNP/GCE the increase was much less, of 19 and 6 times, respectively.

The peak shift is clear evidence of the electrocatalytic effect towards TP oxidation, which may be partly attributed to some oxygen-containing groups on the MWCNT surface (introduced during functionalization in acid media)[28,29] and by the addition of the gold nanoparticles. The high effective electrostatic interaction promoted between TP and surface modified electrode greatly contributes to the observed electrocatalytic effect. The additional increase in electroactive area and in conductivity on introducing AuNP explains the increased current. The increase in the background current at AuNP–MWCNT$_{0.25}$/GCE implies that the effective surface area increases significantly

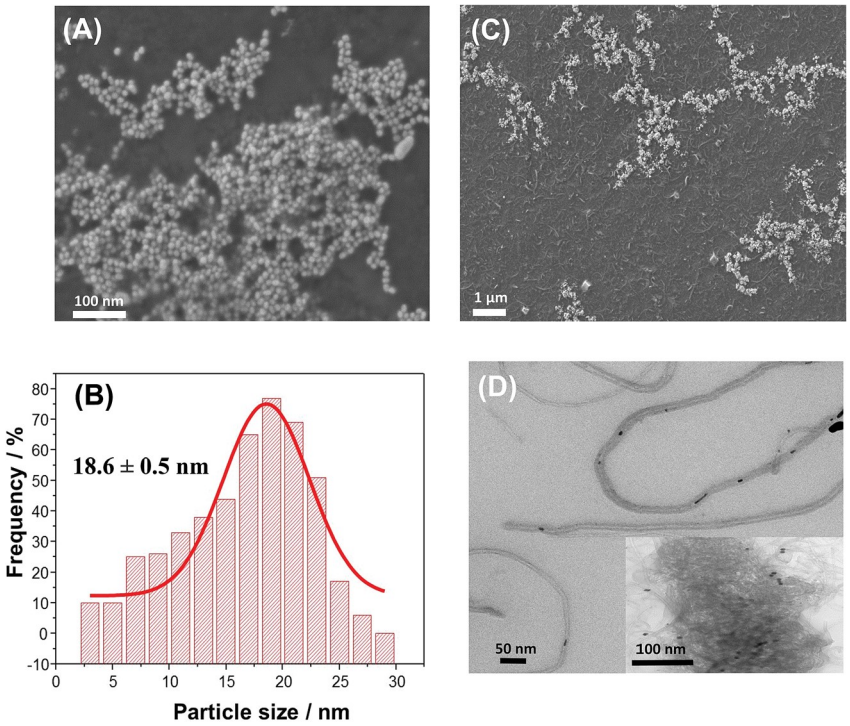

Fig. 1 (A) SEM image showing the morphology and distribution of the AuNP synthesized and stabilized by sodium citrate; (B) size distribution histogram of the AuNP diameter; (C) SEM image of MWCNT decorated by AuNP; (D) TEM image of individual MWCNT decorated by AuNP; inset shows network of decorated MWCNT.

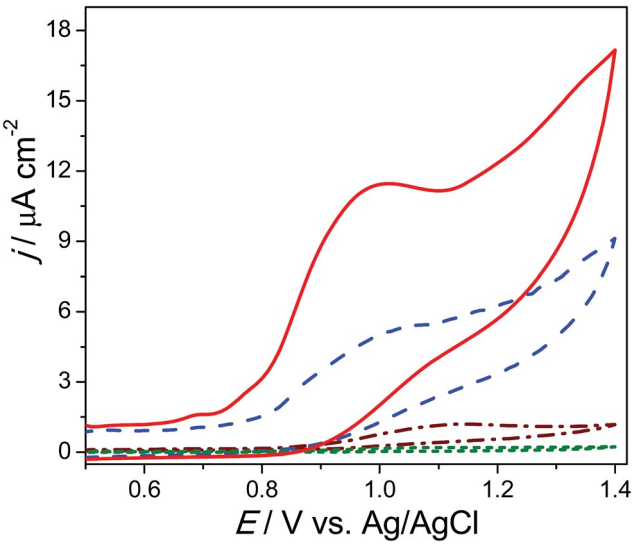

Fig. 2 Cyclic voltammograms for the oxidation of 250 µM TP at different electrode assemblies: (▬ ▬ ▬) GCE; (▬ ▬ ▬) AuNP/GCE; (▬ ▬ ▬) $MWCNT_{0.25}$/GCE; (▬▬▬) AuNP–$MWCNT_{0.25}$/GCE.

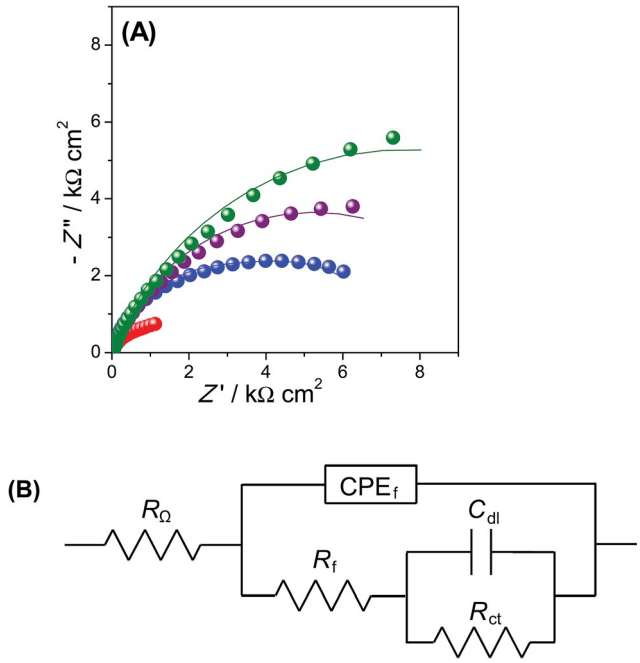

Fig. 3 (A) Electrochemical impedance spectra at: (●) GCE, (●) AuNP/GCE, (●) $MWCNT_{0.25}$/GCE and (●) AuNP–$MWCNT_{0.25}$/GCE in the presence of 250 µM TP in BR pH 6.0 at +1.0 V *vs.* Ag/AgCl. (B) Equivalent electrical circuit used for fitting the impedance spectra.

after modification in comparison with the other electrode assemblies studied. It was verified that in the second sweep, the peak current decreased greatly and this is associated with adsorption of TP's oxidation product at the electrode surface. The voltammograms presented in Fig. 2 are those corresponding to the first cycle.

3.2.2. Electrochemical impedance spectroscopy. Electrochemical impedance spectroscopy was used to characterize the physical and interfacial properties of the different modified electrodes, Fig. 3A. The spectra were recorded at bare GCE, AuNP/GCE, $MWCNT_{0.25}$/GCE, AuNP–$MWCNT_{0.25}$/GCE, in the presence of 250 µM TP prepared in BR buffer solution, pH 6.0 at +1.0 V *vs.* Ag/AgCl. As can be seen, all spectra had the shape of part of a semicircle and were fitted with the same electrical circuit, except for that of bare electrodes, which was simpler. The circuit used to fit all the spectra, except for bare electrodes, is that illustrated in Fig. 3B. It consists of a cell resistance (R_Ω) in series with two parallel combinations, one containing a constant phase element (CPE) and a resistance (R) and the other the same, but except that instead of a CPE a capacitor (C) was used. For high frequencies, the constant phase element and resistance are associated with the process occurring at the interface electrode/modifier film and inside the modifier film, CPE_f and R_f, respectively. For low frequencies, the capacitor and resistance describe the modifier film/solution interface and correspond to the double layer capacitance C_{dl} and charge transfer resistance, R_{ct}, respectively. For bare electrodes only, one parallel combination was used in series with R_Ω, describing solely the interface of the electrode with solution. The CPE is modelled as a non-ideal capacitor and is given by $CPE = -1/(i\omega C)^\alpha$, where C is the capacitance, ω is the frequency in rad s^{-1}, and the exponent α reflects the surface non-uniformity and porosity of the modified electrode assembly, where $\alpha = 1$ correspond to a perfect uniform and smooth surface.[30] The cell resistance is ~16 Ω cm^2 in all cases, and for bare electrodes the R_{ct} = 15.5 kΩ cm^2, C_{dl} = 312 µF cm^{-2} $s^{\alpha-1}$ and α = 0.77; for modified electrodes the parameter values are shown in Table 1.

For all modified electrodes there is a big decrease in charge transfer resistance values compared with bare electrodes, attributed to easier electron transfer as well as increased surface area; they follow the order R_{ct}(GCE) > R_{ct}(AuNP/GCE) > R_{ct}($MWCNT_{0.25}$/GCE) > R_{ct}(AuNP–$MWCNT_{0.25}$/GCE), showing that the fastest electron exchange occurs at AuNP–$MWCNT_{0.25}$/GCE. This is in agreement with the CV experiments, in which the sensor prepared with AuNP–$MWCNT_{0.25}$ modified GCE presented the best performance for theophylline measurement. The R_{ct} decrease is accompanied by an increase in C_{dl}, due to a greater charge separation at modified electrodes. Regarding the film capacitance, its values increase with each modification of the electrode, reaching a maximum at AuNP–$MWCNT_{0.25}$, showing the highest charge accumulation at this electrode assembly. On the contrary, the film resistance decreases, indicating a lower polarisation at AuNP–$MWCNT_{0.25}$/GCE. The value of the exponent α increases with modification, indicating a smoother surface compared with bare electrodes.

3.3. Electrochemical behaviour of theophylline at modified electrode

3.3.1. Effect of scan rate. The electrochemical behaviour of 250 µM TP in BR buffer (pH 6.0) at GCE modified with AuNP–$MWCNT_{0.25}$ was investigated by cyclic voltammetry at different scan rates, Fig. 4A. There is a linear relationship between peak current and scan rate, ν, between 5 and 100 mV s^{-1} (not shown), indicating a surface-confined process[31] expressed by:

Table 1 Equivalent circuit element values obtained by fitting of the impedance spectra from Fig. 3 for different electrode configurations

Electrode configuration	R_f/kΩ cm^2	C_f/μF cm^{-2} s$^{\alpha-1}$	α_f	R_{ct}/kΩ cm^2	C_{dl}/mF cm^{-2}
AuNP/GCE	7.28	330	0.82	2.66	1.08
MWCNT$_{0.25}$/GCE	5.35	437	0.85	1.93	2.58
AuNP–MWCNT$_{0.25}$/GCE	1.33	1190	0.85	1.04	6.00

$$I_p\ (\mu A) = 38.2\nu - 0.48,\ r = 0.9976 \quad (1)$$

In addition, a plot of log I_p *versus* log ν (Fig. 4B), is linear according to

$$\log I_p = 1.06 \log \nu + 3.05,\ r = 0.9989 \quad (2)$$

the slope of 1.06 is close to the theoretically expected value of 1.0 attributed to a purely adsorption controlled process.[31]

The adsorption of TP at AuNP–MWCNT$_{0.25}$ was also experimentally verified in cyclic voltammetry (see ESI, Fig. S2†) when performing consecutive scans in which a gradual decrease of peak current with the number of scans was observed. After carrying out CV in the presence of TP, the modified electrode was cycled in buffer solution without TP and the peak corresponding to TP was seen, also indicating adsorption at the modified electrode.

3.3.2. Influence of pH. The effect of solution pH on the oxidation of TP was investigated by DPV in the pH range from 4.0 to 9.0 (Fig. 5A). There was an increase of oxidation peak current from pH 4.0 to 6.0, followed by a decrease from pH 6.0 to 9.0, Fig. 5B. An explanation of this behaviour is the following. In the pH range investigated, TP molecules in the solution are mostly protonated (pK_a = 8.8)[32] and the surface of the modified electrode is rich in negative charges from AuNP, as well as from carboxyl groups from MWCNT. With the increase of pH, the extent of positive charging at TP is decreasing, leading to a decrease in the effective electrostatic interaction between the TP and the modified electrode. This causes a drop in the peak current at higher pH values.[33] In light of these results, pH 6.0 was selected as the optimum pH value for TP determination.

With increasing solution pH from 4.0 to 9.0, the oxidation peak potential (E_{pa}) shifted negatively and linearly, according to the equation: $E/V = 1.37 - 0.058$ pH ($r = 0.9991$) with a slope of ≅58 mV pH^{-1}, indicating an equal number of protons and electrons participating in the oxidation process.

3.3.3. Oxidation mechanism. The electrode reaction was irreversible, as revealed by the lack of reduction peak in the cyclic voltammograms as well as by the peak potential shifting to positive values with increasing scan rate. There was a linear dependence between peak potential and logarithm of scan rate (Fig. 4C) according to:

$$E_{pa} = 0.036 \log \nu + 1.09,\ r = 0.9956 \quad (3)$$

Since the oxidation reaction of TP is an irreversible process, Laviron's equation,[34] gives the slope of the plot as $2.303RT/(\alpha_a nF)$ where R is the gas universal constant, T is the temperature in K, α_a is the anodic charge transfer coefficient, n is the number of electrons transferred, and F is the Faraday constant. At 25 °C, the value of $\alpha_a n$ was calculated to be 1.15. It can thus be inferred that the number of electrons is 2, with α_a 0.58, in agreement with.[22,32,35–38]

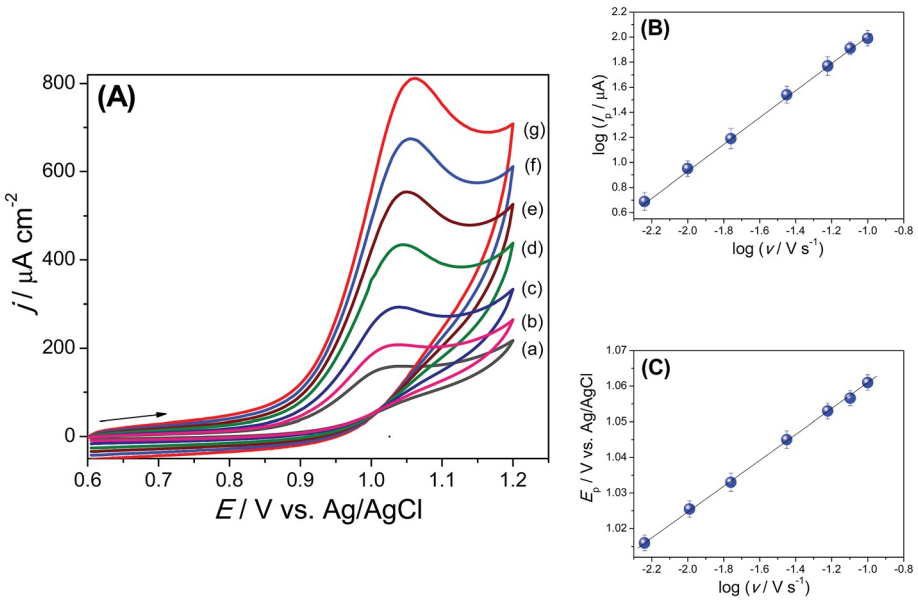

Fig. 4 (A) Cyclic voltammograms for the oxidation of 250 μM TP at AuNP–MWCNT$_{0.25}$/GCE at different scan rates: (a) 5; (b) 10; (c) 20; (d) 40; (e) 60; (f) 80; (g) 100 mV s^{-1}. Influence of logarithm of scan rate on the (B) logarithm of peak current and (C) peak potential.

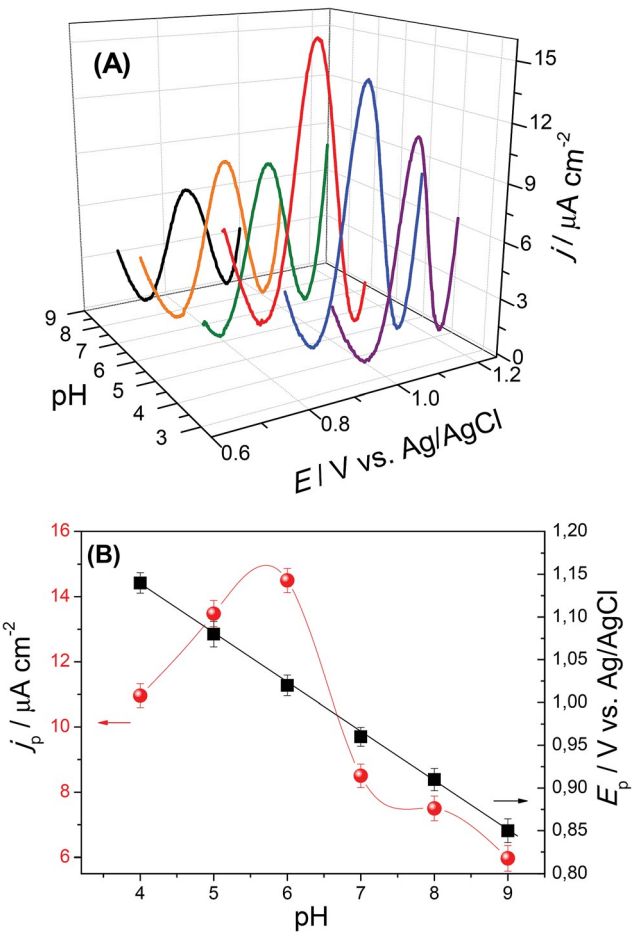

Fig. 5 (A) Differential pulse voltammograms of 5 μM TP at AuNP–$MWCNT_{0.25}$/GCE in BR buffer at different pH values; (B) effect of pH on the TP oxidation peak current and peak potential.

A possible mechanism for protonated TP oxidation at the pH values used here is given in Scheme 1.[38] The proposed mechanism involves a 2-electrons and 2-proton oxidation of an aromatic carbon sandwiched between electron-withdrawing nitrogen heteroatoms, as is the case of the structurally similar guanine. Therefore, the formation of the carbonyl is more likely.[39]

3.4. Electrochemical determination of TP at AuNP–MWCNT-modified GCE

The electrochemical detection of TP was carried out by DPV, which exhibits a higher sensitivity for analytical measurements than CV, and with a lower background current. Based on previous optimisation, a BR buffer solution of pH 6.0 was selected as the supporting electrolyte for the quantification of TP.

It is well known that the oxidation product of theophylline has a very strong tendency to adsorb passivating the electrode surface. It has been suggested that pre-concentration of the analyte can overcome this problem.[37,40–42] Thus, experiments involving pre-concentration were performed, with a view to enhancing the sensitivity, decreasing the detection limit and avoiding problems arising from product adsorption. Accumulation was done at potential values in the range from +0.3 to +1.2 V during 200 s, in intervals of 0.1 V and for accumulation times of 20, 50, 60, 80, 100, 120, 150, 200, 210 and 250 s. A maximum peak current was found for an accumulation potential of +0.7 V. It is at this potential that probably enough species are attracted to the electrode surface, as observed from Fig. 2; this is the potential where oxidation begins. This potential ensures the maximum energy necessary for a greater electrostatic interaction between the positive charges of the TP and the negatively charged carboxyl groups on the carbon nanotubes, which were introduced during the acidic functionalization. The effect of accumulation time on TP oxidation showed an increase in the oxidation peak current up to 200 s; above this time no additional increase was observed. Thus, 200 s was taken as the optimum value and used in further experiments.

The performance of AuNP–MWCNT modified glassy carbon electrodes was investigated by using different loadings of MWCNT in the dispersion solution with AuNP. The determination of TP at these different electrode configurations is presented in Table 2. The sensitivity increased with increase in MWCNT concentration; the highest sensitivity being achieved at AuNP–$MWCNT_{0.50}$/GCE. However, this electrode presented the narrowest linear range and the highest limit of detection, LOD = 3.3(SD/slope),[43] about 4 times higher than that obtained at AuNP–$MWCNT_{0.25}$/GCE. This is probably due to a diffusion barrier caused by increased film thickness. The widest linear range and the lowest detection limit were attained at AuNP–

Table 2 Analytical parameters for determination of TP at different electrode assemblies in BR buffer solution, pH 6

Electrode configuration	Linear range/μM	Sensitivity/μA cm^{-2} μM^{-1}	LOD/μM
GCE	0.5–6.0	0.48	0.50
AuNP–$MWCNT_{0.10}$/GCE	0.5–10	0.32	0.27
AuNP–$MWCNT_{0.25}$/GCE	0.5–20	1.32	0.09
AuNP–$MWCNT_{0.50}$/GCE	2.0–20	1.79	0.36

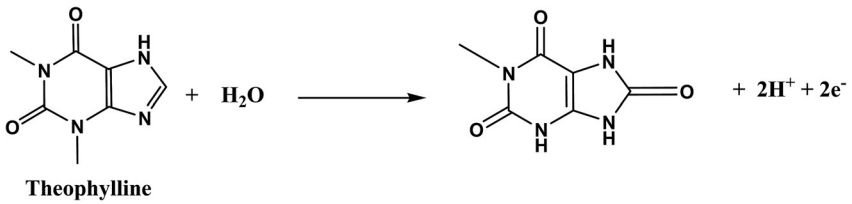

Scheme 1 Possible reaction mechanism for electrooxidation of TP, see ref. 38.

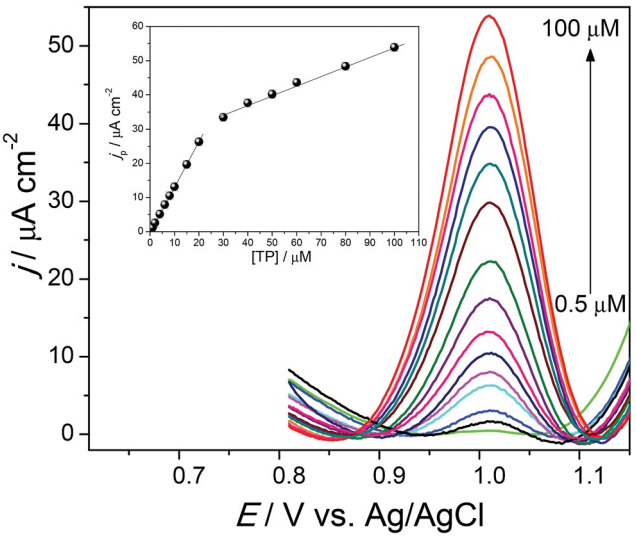

Fig. 6 Differential pulse voltammograms at AuNP–MWCNT$_{0.25}$/GCE in BR, pH 6.0 containing different concentrations of TP.

MWCNT$_{0.25}$/GCE. This electrode exhibited also the second highest sensitivity. Taking into account the results obtained, this last configuration was chosen as optimum for further studies.

Differential pulse voltammograms obtained with increasing TP concentrations at AuNP–MWCNT$_{0.25}$/GCE are shown in Fig. 6. The oxidation peak current increased linearly with theophylline concentration in the ranges of 0.5–20 μM and 30–40 μM with a detection limit of 90 nM determined from the first linear range. The equations for the linear range were j_p (μA cm^{-2}) = 1.32C − 0.12 (r^2 = 0.999, C is in μM) and j_p (μA cm^{-2}) = 0.28C + 25.89 (r^2 = 0.997, C is in μM). In the second range, a decrease of the sensitivity (slope) was observed due to kinetic limitations which may be attributed to the adsorption of TP's oxidation product on the electrode surface.[44] A comparison of the proposed electrode configuration for TP determination with other similar electrochemical platforms[22–24,37,45–51] using voltammetric techniques is given in Table 3. It can be seen that the new method for preparation of AuNP–MWCNT modified GCE offered a reasonable linear range for TP determination and the low detection limit is comparable with others or even smaller and especially much smaller than the 2.0 μM achieved at similar architecture electrode with carbon nanotubes and gold nanoparticles plus poly-L-lysine.[24] Furthermore, the proposed sensor offers several advantages compared with other modified electrodes for TP determination, especially less complex architecture and rapid preparation, and lower detection potential. There is only one report of a lower potential than here,[23] but it required an ionic liquid.

3.5. Repeatability and stability at AuNP–MWCNT/GCE

The repeatability of the AuNP–MWCNT$_{0.25}$/GCE electrode was investigated by measuring the response to 250 μM TP in BR, pH 6.0; the RSD was 3.9% with 20 successive measurements. The long-term stability of the electrode was investigated by recording its response to 250 μM TP over 45 days. When not in use, the electrode was stored at room temperature in a dark environment. After 45 days the current response of the sensor remained at 92% (3 sensors), which is better than that achieved in.[22,39] The results above revealed a high stability and a good reproducibility and repeatability of AuNP–MWCNT$_{0.25}$/GCE for TP determination.

3.6. Interferences

Under the optimum experimental conditions, the effect of potential interferents on the DPV response of 250 μM TP was evaluated by measuring the peak current corresponding to TP oxidation in the absence and presence of foreign species. The results are listed in Table 4.

It was found that 50-fold higher concentrations of glucose, xanthine, hydroquinone, sucrose and 100-fold of Zn^{2+}, Mg^{2+}, K^+, SO_4^{2-}, do not interfere with the oxidation signal of TP (signal change less than 8%) in agreement with the literature.[30,36,46]

Table 3 Comparison of the TP determination performance of AuNP–MWCNT$_{0.25}$/GCE with other electrode configurations[a]

Modified electrode configuration	Technique	Peak potential/V	pH	E_{acc}/V;t_{acc}/s	Linear range/μM	Sensitivity/μA cm^{-2} μM^{-1}	LOD/nM	Ref.
MWCNT-CPE	DPV	1.20 (Ag/AgCl)	3.0	OCP; 10	2.0–150	[b]	20	22
MWCNT-IL/GCE	DPV	0.83 (Ag/AgCl)	7.0	—	0.5–98	[b]	160	22
MWCNT/AuNP/PLL/SPE	SWV	0.98 (SPE)	7.5	—	10–200	[b]	2000	24
MWCNT/GCE	CV	1.08 (SCE)	5.8	OCP; 120	0.3–10	[b]	50	35
PAV3B/MWCNT/Gr/GCE	DPV	1.15 (SCE)	4.5	—	0.5–120	6.56	20	45
MnO_2/MWCNT/GCE	DPV	1.05 (SCE)	6.0	—	0.1–20	66.2	10	46
AT–AuNP/GCE	DPV	1.07 (Ag/AgCl)	6.0	—	20–240	0.38	—	47
PtNP/MWCNT-IL/GCE	CV	1.1 (SCE)	3.0	OCP; 120	0.01–10	46.1	8	48
PCys/N-CNT/GCE	DPV	1.17 (SCE)	1.7	—	0.1–70	1.23	33	49
MnO_2-IL-Gr/GCE	DPV	1.1 (Ag/AgCl)	5.0	—	1.0–10	[b]	100	50
PFA/Gr/GCE	DPV	1.18 (SCE)	4.5	—	0.2–10	4.84	30	51
AuNP-MWCNT$_{0.25}$/GCE	DPV	0.98 (Ag/AgCl)	6.0	+0.7; 200	0.5–20	1.32	90	This work

[a] CPE – carbon paste electrode, SPE – screen printed electrode, PLL – poly-L-lysine, PAV3B – poly(Alizarin Violet 3B); Gr – graphene, AT – aminotriazole, IL – ionic liquid, PtNP – platinum nanoparticles; PCys – poly(cysteine); N-CNT – N-doped carbon nanotubes; PFA – poly(folic acid). [b] No electrode area specified.

Table 4 Influence of potential interferents on the voltammetric response to 250 μM TP in BR buffer solution, pH 6.0

Interferents	Ratio [interferent : TP]	Signal change/%
Glucose	50 : 1	+3.1
Xanthine	50 : 1	−6.1
Hydroquinone	50 : 1	−8.1
Sucrose	50 : 1	+1.1
Zn^{2+}	100 : 1	−3.1
Mg^{2+}	100 : 1	+4.3
K^{+}	100 : 1	+4.9
SO_4^{2-}	100 : 1	−5.8

Table 5 Determination of TP in commercial samples

Samples	Original (μM)	Added (μM)	Found (μM)	Recovery (%)
TP tablets	2.26	1.00	3.39	104.0 ± 6.0
Black tea	1.37	1.00	2.40	101.3 ± 4.0
Green tea	1.13	1.00	2.18	102.3 ± 5.0

3.7. Determination of TP in commercial samples

In order to investigate the applicability of the proposed method, the AuNP–$MWCNT_{0.25}$/GCE was used for TP determination in commercial samples of TP tablets, green tea and black tea purchased from local market and used for quantitative analysis after preparation as described in the Experimental section. Each sample was measured in triplicate, using the standard addition method and the results are summarized in Table 5. The quantity of theophylline found in the original samples is given as the value obtained in the cell after dilution; in case of the teas a 1 : 20 and for the tablet a 1 : 1000 dilution was applied. From the results in Table 5, the detected content of TP was calculated as 407 mg per tablet ($n = 3$), which is 101.7% of the labelled value (400 mg per tablet). The concentration of TP in the green tea and black tea were calculated as 4.07 and 5.93 mg L^{-1} respectively, which is comparable with values found in the literature.[40,41] The recoveries were in the range of 101.3% to 104.0% with RSD less than 10%, which clearly indicates the applicability and reliability of the proposed method.

4. Conclusions

A novel and simple electrode configuration based on AuNP dispersed on MWCNT–chitosan network deposited in one step on CGE substrate is proposed to investigate the electrochemical behaviour of TP. From the architectures studied here, AuNP–$MWCNT_{0.25}$/GCE showed the best electrocatalytic effect for the oxidation of TP, exhibiting the highest enhancement of the oxidation peak current, which can be attributed to the larger effective surface area and the synergetic effect obtained by the efficient aggregation of AuNP on MWCNT network that increased greatly the conductivity. The developed sensor showed similar performance to other modified electrodes but offers the important advantages of lower detection potential, easy and fast preparation and less complex architecture. Finally, the new sensor has also been successfully applied to determine TP in commercial samples with very good recoveries, which indicates its application to therapeutic drug monitoring of TP and in the quality control of tea.

Conflicts of interest

There are no conflicts to declare.

Acknowledgements

The authors are grateful for financial support from Fundação para a Ciência e a Tecnologia (FCT), Portugal projects PTDC/QEQ-QAN/2201/2014, in the framework of Project 3599-PPCDT, and UID/EMS/00285/2013 (both co-financed by the European Community Fund FEDER). MEG thanks FCT for a postdoctoral fellowship SFRH/BPD/103103/2014 and WS thanks the Conselho Nacional de Desenvolvimento Científico e Tecnológico (CNPq), Brazil for a doctoral fellowship, 232979/2014-6.

References

1 G. Yang, F. Zhao and B. Zeng, *Talanta*, 2014, **127**, 116–122.
2 J. Wang, *Microchim. Acta*, 2012, **177**, 245–270.
3 V. Pifferi, V. Marona, M. Longhi and L. Falciola, *Electrochim. Acta*, 2013, **109**, 447–453.
4 H. Hosseini, M. Behbahani, M. Mahyari, H. Kazerooni, A. Bagheri and A. Shaabani, *Biosens. Bioelectron.*, 2014, **59**, 412–417.
5 A. Ananthi and K. L. Phani, *J. Electroanal. Chem.*, 2016, **764**, 7–14.
6 H. Cheng, J. Liang, Q. Zhang and Y. Tu, *J. Electroanal. Chem.*, 2012, **674**, 7–11.
7 A. A. Rafati and A. Afraz, *Mater. Sci. Eng., C*, 2014, **39**, 105–112.
8 R. Y. Zhang and H. Olin, *Int. J. Biomed. Nanosci. Nanotechnol.*, 2011, **2**, 112.
9 H.-F. Cui, Y.-H. Cui, Y.-L. Sun, K. Zhang and W.-D. Zhang, *Nanotechnology*, 2010, **21**, 215601.
10 Y. Shi, R. Yang and P. K. Yuet, *Carbon*, 2009, **47**, 1146–1151.
11 F. Jia, C. Shan, F. Li and L. Niu, *Biosens. Bioelectron.*, 2008, **24**, 945–950.
12 Z. Wang, H. Guo, R. Gui, H. Jin, J. Xia and F. Zhang, *Sens. Actuators, B*, 2018, **255**, 2069–2077.
13 S. Shahrokhian and M. Hafezi-Kahnamouei, *J. Electroanal. Chem.*, 2018, **825**, 30–39.
14 M. A. Tahir, S. Z. Bajwa, S. Mansoor, R. W. Briddon, W. S. Khan, B. E. Scheffler and I. Amin, *J. Hazard. Mater.*, 2018, **346**, 27–35.
15 E. E. Ferapontova, E. M. Olsen and K. V. Gothelf, *J. Am. Chem. Soc.*, 2008, **130**, 4256–4258.
16 M. Zydron, J. Baranowska and I. Baranowska, *J. Sep. Sci.*, 2004, **14**, 1166–1172.
17 P. D. Tzanavaras, C. K. Zacharis and D. G. Themelis, *Talanta*, 2010, **81**, 1494–1501.

18 K. Saka, K. Uemura, K. Shintani-Ishida and K. Yoshida, *J. Chromatogr. B: Anal. Technol. Biomed. Life Sci.*, 2007, **846**, 240–244.
19 V. Zare-Shahabadi, M. Shamsipur, B. Hemmatenejad and M. Akhond, *Anal. Lett.*, 2010, **43**, 687–700.
20 R. Hajian, N. Shams and Z. Davarpanah, *E-J. Chem.*, 2011, **8**, 966–976.
21 S. Güney and F. Cebeci, *Sens. Actuators, B*, 2015, **208**, 307–314.
22 S. J. Malode, N. P. Shetti and S. T. Nandibewoor, *Colloids Surf., B*, 2012, **97**, 1–6.
23 M. B. Gholivand and M. Khodadadian, *Electroanalysis*, 2014, **26**, 1975–1983.
24 A. Peng, H. Yan, C. Luo, G. Wang, X. Ye and H. Ding, *Int. J. Electrochem. Sci.*, 2017, **12**, 330–346.
25 V. Shakila and K. Pandian, *J. Solid State Electrochem.*, 2007, **11**, 296–302.
26 M. E. Ghica and C. M. A. Brett, *Anal. Lett.*, 2013, **46**, 1379–1393.
27 K. N. Rathod, Z. Joshi, D. Dhruv, K. Gadani, H. Boricha, A. D. Joshi, P. S. Solanki and N. A. Shah, *Mater. Res. Express*, 2018, **5**, 1–10.
28 M. Musameh, J. Wang, A. Merkoci and Y. Lin, *Electrochem. Commun.*, 2002, **4**, 743–746.
29 H. Luo, Z. Shi, N. Li, Z. Gu and Q. Zhuang, *Anal. Chem.*, 2001, **73**, 915–920.
30 M. E. Ghica and C. M. A. Brett, *J. Electroanal. Chem.*, 2009, **629**, 35–42.
31 C. M. A. Brett and A. M. Oliveira Brett, *Electrochemistry. Principles, Methods and Applications*, Oxford University Press, Oxford, 1993.
32 L. Zi, J. Li, Y. Mao, R. Yang and L. Qu, *Electrochim. Acta*, 2012, **78**, 434–439.
33 M. Mazloum-Ardakani, H. Beitollahi, B. Ganjipour, H. Naeimi and M. Nejati, *Bioelectrochemistry*, 2009, **75**, 1–8.
34 E. Laviron, *J. Electroanal. Chem.*, 1979, **101**, 19–28.
35 M. Amare and S. Admassie, *Bull. Chem. Soc. Ethiop.*, 2012, **26**, 73–84.
36 R. R. H. Rajesh, N. Hegde and S. T. Nandibewoor, *Anal. Lett.*, 2009, **42**, 2665–2682.
37 Y. H. Zhu, Z. L. Zhang and D. W. Pang, *J. Electroanal. Chem.*, 2005, **581**, 303–309.
38 T. Wang, E. P. Randviir and C. E. Banks, *Analyst*, 2014, **139**, 2000–2003.
39 R. N. Goyal and A. Dhawan, *J. Electroanal. Chem.*, 2006, **591**, 159–167.
40 H. Yin, X. Meng, H. Su, M. Xu and S. Ai, *Food Chem.*, 2012, **134**, 1225–1230.
41 J. M. Zen, T. Y. Yu and Y. Shih, *Talanta*, 1999, **50**, 635–640.
42 R. N. Hedge, R. R. Hosamani and T. S. Nandibewoor, *Anal. Lett.*, 2009, **42**, 2665–2682.
43 C. M. A. Brett and A. M. Oliveira Brett, *Electroanalysis*, Oxford University Press, Oxford, 1998.
44 S. J. Malode, J. C. Abbar, N. P. Shetti and S. T. Nandibewoor, *Electrochim. Acta*, 2012, **60**, 95–101.
45 Y. Wang, T. Wu and C. yan Bi, *Microchim. Acta*, 2016, **183**, 731–739.
46 Y. J. Yang and W. Li, *Ionics*, 2015, **21**, 1121–1128.
47 S. Kesavan and S. Abraham John, *Sens. Actuators, B*, 2014, **205**, 352–362.
48 L. Liu, F. Xiao, J. Li, W. Wu, F. Zhao and B. Zeng, *Electroanalysis*, 2008, **20**, 1194–1199.
49 Y. Wang, Y. Ding, L. Li and P. Hu, *Talanta*, 2018, **178**, 449–457.
50 X. Zhuang, D. Chen, S. Wang, H. Liu and L. Chen, *Sens. Actuators, B*, 2017, **251**, 185–191.
51 X. Shu, F. Bian, Q. Wang, X. Qin and Y. Wang, *Int. J. Electrochem. Sci.*, 2017, **12**, 4251–4264.

Electronic Supplementary Material (ESI) for Analytical Methods.

SUPPLEMENTARY MATERIAL

GOLD NANOPARTICLE DECORATED MULTIWALLED CARBON NANOTUBE MODIFIED ELECTRODES FOR THE ELECTROCHEMICAL DETERMINATION OF THEOPHYLLINE

Wanderson da Silva, Mariana Emilia Ghica, Christopher M.A. Brett

Department of Chemistry, Faculty of Sciences and Technology, University of Coimbra, 3004-535 Coimbra, Portugal

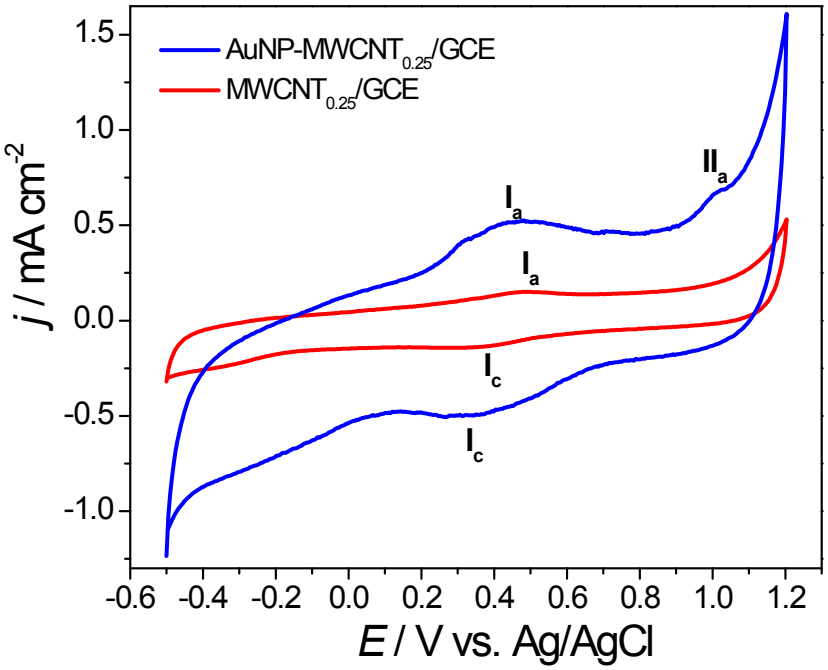

Figure S1. Cyclic voltammogram at (blue) AuNP-$MWCNT_{0.25}$/GCE and (red) $MWCT_{0.25}$/GCE in 0.1 M H_2SO_4. Scan rate 100 mV s^{-1}.

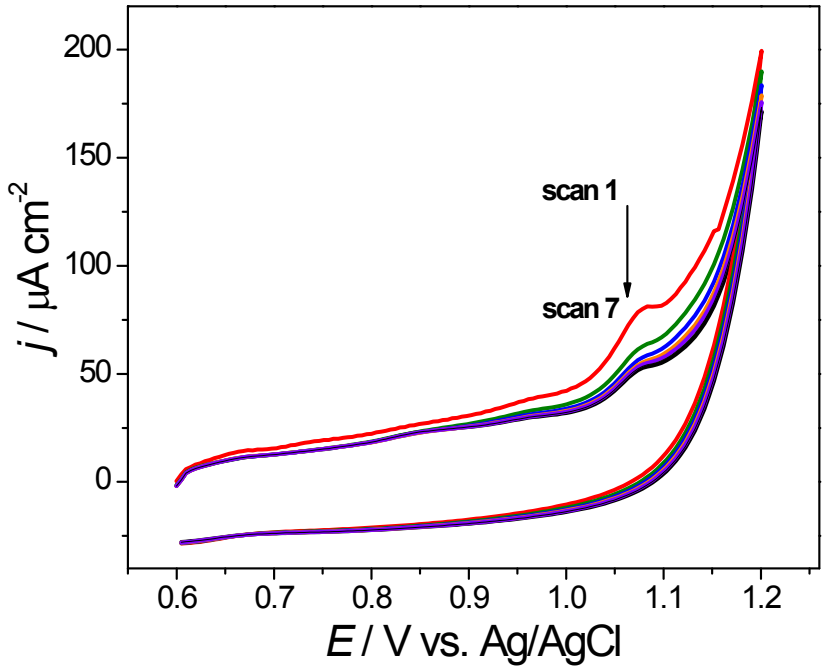

Figure S2. Consecutive cyclic voltammograms at AuNP-MWCNT$_{0.25}$/GCE with 50 μM TP in 0.1 M BR buffer solution, pH 6.0, scan rate 100 mV s^{-1}.